# Multiple-particle interaction in (1 + 1)-dimensional lattice model

Peng Guo[1,2,*] and Tyler Morris[1]

[1]Department of Physics and Engineering, California State University, Bakersfield, California 93311, USA
[2]Kavli Institute for Theoretical Physics, University of California, Santa Barbara, California 93106, USA

(Received 22 August 2018; published 2 January 2019)

Finite volume multiple-particle interaction is studied in a two-dimensional complex $\phi^4$ lattice model. The existence of analytical solutions to the $\phi^4$ model in two-dimensional space and time makes it a perfect model for the numerical study of finite volume effects of multiparticle interaction. The spectra from multiple particles are extracted from the Monte Carlo simulation on various lattices in several moving frames. The $S$-matrix of multiparticle scattering in $\phi^4$ theory is completely determined by two fundamental parameters: single-particle mass and the coupling strength of two-to-two particle interaction. These two parameters are fixed by studying single-particle and two-particle spectra. Due to the absence of the diffraction effect in the $\phi^4$ model, three-particle quantization conditions are given in a simple analytical form. The three-particle spectra from simulation show remarkable agreement with the prediction of exact solutions.

DOI: 10.1103/PhysRevD.99.014501

## I. INTRODUCTION

One of the outstanding but challenging goals in nuclear/hadron physics is to understand the dynamics of particle interaction. Multiple-particle interaction is not only important to nuclear/hadron physics, but also plays a crucial role in astrophysics, atomic, and condensed matter physics. However, the complication increases dramatically with increasing numbers of dynamical degrees of freedom and poses a significant obstacle in studying and understanding multiparticle interaction. Fortunately, the simplest case of multiparticle interaction turns out to be manageable, three-particle interaction. The dynamics of three-particle interaction were well developed and studied in the past [1–20]. Recent progress in high statistic experiments, such as GlueX and CLAS programs, has triggered renewed interest in three-body dynamics. One example is the extraction of the $u$- and $d$-quark mass difference from the $\eta \to 3\pi$ decay process [21–28]. On the other hand, lattice QCD provides an unprecedented opportunity for the study of multiple-particle interaction from the heart of hadrons with quarks and gluons as the fundamental building blocks. Recent advances in lattice computation have made the study of hadron interaction especially possible [29–40]. Because lattice QCD is formulated in Euclidean space, access to scattering information is not always direct. That adds some additional complication in multiparticle studies in lattice QCD as well as the intense numerical computation and other difficulties. A formalism was proposed nearly 30 years ago by Lüscher [41] to tackle the two-particle elastic scattering problem in a finite volume; it is known as the Lüscher formula. Since then, the framework was quickly extended to moving frames [42–46] and to coupled-channel scattering [47–53]. In the three-particle sector, many groups have made remarkable progress [54–70] related to the theoretical algorithm of extracting scattering amplitudes from lattice data in recent years.

A three-particle lattice simulation was recently performed based on a complex $\phi^4$ toy model [71]; the data analysis was carried out by adopting the effective theory framework. However, the simulation and analysis are limited solely to ground state energy levels where all three particles are nearly at rest, and the three-particle signals are quite noisy. In the present work, we aim to perform a simulation on multiple-particle interaction also using the $\phi^4$ model and study the finite volume effect on multiple-particle spectra in a better-controlled environment and a more systematic way. For this purpose, multiple numbers of multiparticle operators are used in our simulation, and variational analysis [72–74] is implemented to extract excited state energy levels. The exact scattering solutions of $\phi^4$ theory in $(1 + 1)$ dimensions are known in both free space [75–77] and a finite volume [64]. Taking advantage of existing analytic multiple-particle scattering solutions, we therefore perform the simulation in $(1 + 1)$-dimensional space and time for various lattice sizes and moving frames. The exact scattering solutions are used in the data analysis of multiparticle simulation. In principle, the multiple-particle scattering $S$-matrices are completely determined

*pguo@csub.edu

by only two free parameters: the single-particle mass and the coupling strength of two-to-two particle interaction. The single-particle mass is obtained from single-particle correlation functions, and the coupling strength of pairwise interaction is extracted by studying two-particle scattering spectra in a lattice. The comparison between three-particle scattering spectra and predicted three-particle energies by using the analytic expression of three-particle quantization conditions is presented at the end of the paper.

The paper is organized as follows. The exact solutions of $\phi^4$ theory for two-body and three-body interaction are summarized in Sec. II. The algorithm of the hybrid Monte Carlo simulation of the lattice model and strategy of data analysis are briefly discussed in Sec. III. The construction of multiparticle operators, multiparticle spectra in lattice simulation, and data analysis are described in Sec. IV. The summary and outlook are given in Sec. V.

## II. EXACT SOLUTION OF $\phi^4$ MODEL IN $2D$

In this section, we summarize some results of the two-dimensional $\phi^4$ model. The classical action of the complex $\phi^4$ model in two-dimensional Euclidean space is

$$S = \int d^2x \left[\frac{1}{2}\partial\phi^*\partial\phi + \frac{1}{2}\mu^2|\phi|^2 + \frac{g}{4!}|\phi|^4\right], \quad (1)$$

where $x = (x_0, x_1)$ are temporal and spatial coordinates in two-dimensional Euclidean space, respectively. It is known [75] that the complex $\phi^4$ model in Eq. (1) is equivalent to a nonrelativistic one-dimensional $N$-body interaction problem of particles interacting with pairwise $\delta$-function potentials,

$$H = -\frac{1}{2m}\sum_{i=1}^{N}\frac{\partial^2}{\partial x_{1,i}^2} + V_0\sum_{i<j}\delta(x_{1,i} - x_{1,j}), \quad (2)$$

where $x_{1,i}$ refers to the spatial position of the $i$th particle, and $m$ stands for the mass of identical bosons. The coupling strength of the $\delta$-function potential, $V_0$, differs from the renormalized $g$ in Eq. (1) by a constant factor. The exact solutions of the multiparticle interaction with $\delta$-function potentials were studied and obtained in both free space [75–77] and a finite volume [64]. In fact, the particles interacting with the $\delta$-function potential in $2D$ are only one of a few exactly solvable multiparticle scattering problems. The multiparticle wave function is described completely by the linear superpositions of plane waves with all possible permutations on particle momenta. No new momenta are generated by collisions; all the diffraction effects are canceled out as a consequence of Bethe's hypothesis [78,79]. The multiparticle $S$-matrix therefore is factorized into the product of a number of two-particle scattering amplitudes, as if the process of multiparticle scattering would be a succession of separated elastic two-particle collisions [64].

In a finite volume for two-particle scattering, only one quantization condition is required [64,80],

$$\cot\delta(k) + \cot\frac{\frac{PL}{2} + kL}{2} = 0, \quad (3)$$

where $P = p_1 + p_2$ and $k = \frac{p_1 - p_2}{2}$ denote the center of mass and relative momenta of two particles, respectively. The phase shift $\delta(k)$ for the $\delta$-function potential is given by $\delta(k) = \cot^{-1}(-\frac{2k}{mV_0})$. The $L$ stands for the size of the square box in $2D$, and the center of mass momentum is discretized because of the periodic boundary condition of the lattice: $P = \frac{2\pi}{L}d, d \in \mathbb{Z}$.

For three-body scattering in a finite volume, three quantization conditions are obtained [64]. Only two of them are independent,

$$\begin{aligned}\cot(-\delta(-q_{31}) - \delta(q_{12})) + \cot\frac{PL - p_1L}{2} = 0,\\ \cot(\delta(-q_{23}) + \delta(q_{12})) + \cot\frac{PL - p_2L}{2} = 0,\end{aligned} \quad (4)$$

where all the relative momenta are given in terms of two independent particle momenta: $p_1$ and $p_2$, $q_{31} = \frac{P - 2p_1 - p_2}{2}$, $q_{12} = \frac{p_1 - p_2}{2}$, and $q_{23} = \frac{p_1 + 2p_2 - P}{2}$. The momentum of particle 3 is constrained by momentum conservation, $p_3 = P - p_1 - p_2$. Again, the center of mass momentum of the three-particle is quantized in the periodic box: $P = \frac{2\pi}{L}d, d \in \mathbb{Z}$.

## III. THE LATTICE $\phi^4$ MODEL ACTION

The lattice $\phi^4$ action is obtained from Eq. (1) by replacing the continuous derivative with a discrete difference: $\partial\phi(x) \to \phi(x + \hat{n}) - \phi(x)$, where $\hat{n}$ denotes the unit vector in direction $x_i$ on a periodic square lattice. In addition, by introducing two new parameters, $\mu^2 = \frac{1 - 2\lambda}{\kappa} - 8$ and $g = \frac{6\lambda}{\kappa^2}$, and also rescaling the $\phi$ field by $\phi \to \sqrt{2\kappa}\phi$, we thus obtain

$$\begin{aligned}S(\phi) = -\kappa\sum_{x,\hat{n}}\phi^*(x)\phi(x + \hat{n}) + \text{c.c.}\\ + (1 - 2\lambda)\sum_x|\phi(x)|^2 + \lambda\sum_x|\phi(x)|^4,\end{aligned} \quad (5)$$

where $x = (x_0, x_1)$ now refers to the discrete coordinates of a Euclidean $T \times L$ lattice site.

### A. Hybrid Monte Carlo algorithm

The hybrid Monte Carlo algorithm [81,82] is adopted in our numerical simulation; the complex $\phi^4$ model is treated as a coupled two-component scalar field model,

$\phi = (\phi_0, \phi_1)$. In hybrid Monte Carlo simulation [81,82], an auxiliary Hamiltonian is introduced,

$$H = \frac{1}{2}\sum_x \pi^*(x)\pi(x) + S(\phi), \tag{6}$$

where $\pi = (\pi_0, \pi_1)$ are fictitious conjugate momenta of the $\phi = (\phi_0, \phi_1)$ field. The auxiliary Hamiltonian in Eq. (6) defines the classical evolution of both the $\pi$ and $\phi$ fields over a fictitious time $\tau$ within an interval $[0, \tau]$:

$$\begin{aligned}\phi_i(\tau) &= \phi_i(0) + \int_0^\tau d\tau' \pi_i(\tau'),\\ \pi_i(\tau) &= \pi_i(0) - \int_0^\tau d\tau' \frac{\partial S(\phi(\tau'))}{\partial \phi_i(\tau')}, \quad i = 0, 1.\end{aligned} \tag{7}$$

The trajectory of $(\phi, \pi)$ over the time interval $[0, \tau]$ is determined by the solutions of the motion equations in Eq. (7).

The two pairs of components, $(\phi_0, \pi_0)$ and $(\phi_1, \pi_1)$, are updated alternately for each sweep over an entire lattice. Updating each pair $(\phi_i, \pi_i)$ is followed with the standard hybrid Monte Carlo algorithm:

(i) The trajectory begins with choosing a random distribution of fields $(\phi(\tau), \pi(\tau))$ at initial time $\tau = 0$. The initial conjugate momenta, $\pi_i(0)$, are generated according to the Gaussian probability distribution: $P(\pi_i) \propto e^{-\frac{\pi_i^2}{2}}$.

(ii) Solve the motion equations in Eq. (7) to evolve $(\phi_i(\tau), \pi_i(\tau))$ over the trajectory up to a time $\tau$. The motion equations [Eq. (7)] are solved numerically by the leapfrog method [82].

(iii) Accept the proposed new fields, $(\phi(\tau), \pi(\tau))$, with probability $P_{\rm acc} = {\rm Min}[1, e^{-\triangle H}]$, where $\triangle H = H(\tau) - H(0)$.

The simulations are performed with the choice of the parameters $\kappa = 0.1286$ and $\lambda = 0.01$. The temporal extent of the lattice is fixed at $T = 80$, and the spatial extent of the lattice, $L$, is from 10 up to 45. For each set of lattice size and moving frame, one million measurements are generated. The length of the trajectory is fixed at $\tau = 8$; the $(\phi, \pi)$ fields evolve from $\tau = 0$ up to $\tau = 8$ over 100 discrete steps.

### B. Strategy of data analysis

As already mentioned in Sec. II, the two-dimensional $\phi^4$ model is exactly solvable; the solutions of the model are given in terms of only two free parameters: the particle mass, $m$, and the coupling strength of the $\delta$-function potential, $V_0$. The mass of identical particles, $m$, can be extracted from one-particle spectra of the lattice simulation. The second parameter, $V_0$, can be fixed by two-particle spectra from the simulation. Taking advantage of the existence of exact solutions of the two-dimensional $\phi^4$ model provides an excellent playground and controlled environment for a systematic study of finite volume effects of multiparticle scattering in lattice simulation. In the present work, we are not aiming at obtaining any new fundamental information from three-body spectra, such as the three-body force effect, etc. Instead, after fixing $m$ and $V_0$ from one- and two-particle spectra, we tend to study how well the three-body spectra from simulation match the prediction of exact solutions. In real QCD simulation, the significant difference between simulation results of three-body spectra and prediction based on pairwise interaction may signal the effect of three-body forces or something more fundamental. The present work serves only as a test bed for more realistic future lattice studies of multiparticle interactions.

To accomplish the goal of this work mentioned above, the following steps are taken in the data analysis of the simulation results:

(1) Measure one-particle spectra for various sizes of lattice and moving frames, and extract continuum limit particle mass, $m$, by using the relation [83] $m(L) = m + \frac{c}{\sqrt{L}} e^{-mL}$.

(2) Measure two-particle spectra for various sizes of lattice and moving frames, and extract the coupling strength, $V_0$, from lattice data.

(3) Three-particle spectra are measured for various sizes of lattice and moving frames as well; three-particle spectra are thus compared with predicted three-particle spectra. The predicted three-particle spectra, $E_{3b}^{(d)}(L)$, are given in terms of two independent particle momenta, $p_1$ and $p_2$, by

$$E_{3b}^{(d)}(L) = \sum_{i=1}^{3} \cosh^{-1}(\cosh m + 1 - \cos p_i),$$

where $p_1$ and $p_2$ are the solutions of Eq. (4), and $p_3 = P - p_1 - p_2$.

The particles spectra are extracted by fitting exponential multiparticle correlation functions as a function of time $x_0$: $C(x_0) \propto e^{-Ex_0}$. See the example of one-, two-, and three-particle correlation functions and effective mass, $\ln \frac{C(x_0)}{C(x_0+1)}$, in Figs. 1 and 2, respectively. The construction of multiparticle operators and correlation functions will be explained later in Sec. IV.

## IV. PARTICLES SPECTRA AND DATA ANALYSIS

In this section, we present significant results for multiparticle scattering. Some details on multiparticle operator construction and data analysis are also given.

### A. One-particle spectra

The one-particle spectra are extracted from the exponential decay of the correlation functions

$$C_{1b,n}(x_0) = \langle \tilde{\phi}_n^*(x_0)\tilde{\phi}_n(0)\rangle \propto e^{-E_{1b,n}x_0}, \tag{8}$$

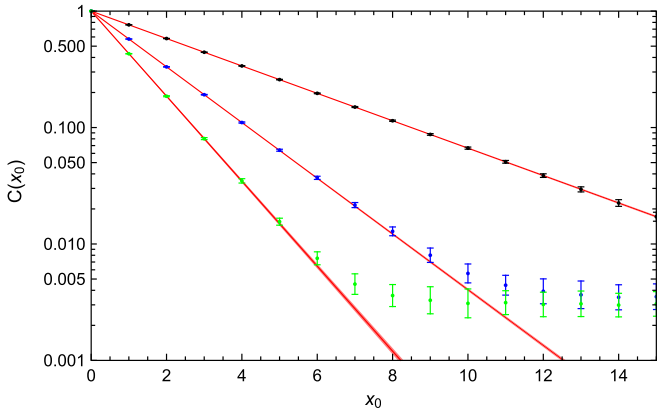


FIG. 1. Correlation functions for one particle (black), two particles (blue), and three particles (green) at $L = 40$ and $P = 0$, and corresponding fitting curves (red band).

where the one-particle propagator, $\tilde{\phi}_n(x_0)$, is defined by

$$\tilde{\phi}_n(x_0) = \frac{1}{L}\sum_{x_1}\phi(x)e^{ix_1\frac{2\pi}{L}n}, \quad n \in \mathbb{Z}. \tag{9}$$

Single-particle energy $E_{1b,n}(L)$ is obtained for multiple lattice sizes, $L = 10$ up to 45. By fitting single-particle energies in multiple lattice sizes with relation

$$m(L) = E_{1b,0}(L) = m + \frac{c}{\sqrt{L}}e^{-mL}, \tag{10}$$

where $c$ and $m$ are used as fitting parameters, we thus find the mass of a single particle: $m = 0.2708 \pm 0.0002$; see Fig. 3. The excited single-particle energy levels are used to check the energy-momentum dispersion relations in a finite lattice,

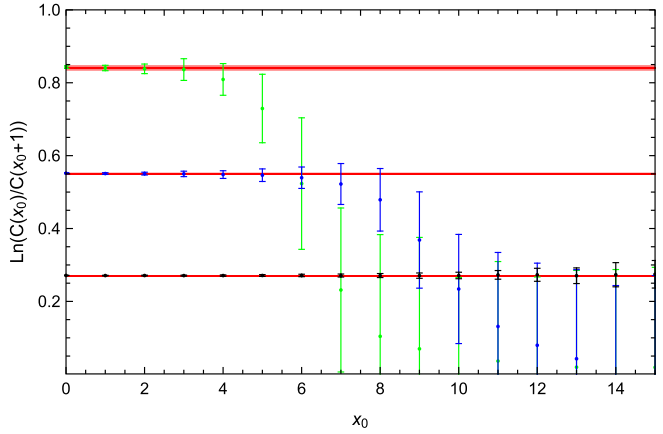


FIG. 2. Effective mass plots, $\ln\frac{C(x_0)}{C(x_0+1)}$, for one particle (black), two particles (blue), and three particles (green) at $L = 40$ and $P = 0$, and corresponding fitting curves (red band).

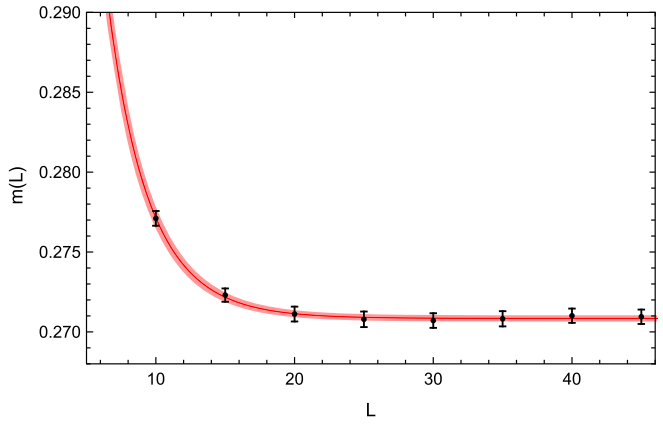


FIG. 3. The single-particle mass spectra $m(L)$ as a function of lattice size $L$. The single-particle mass follows the relation $m(L) = m + c/L^{1/2}e^{-mL}$ (red band).

$$E_{1b,n}(L) = \cosh^{-1}\left(\cosh m + 1 - \cos\frac{2\pi}{L}n\right). \tag{11}$$

The comparison between lattice results and the lattice dispersion relation is presented in Fig. 4.

### B. Two-particle spectra

In moving frames, the matrix elements of the two-particle correlation function read

$$C^{(d)}_{2b,(i,j)}(x_0) = \langle O^{(d)*}_{2b,i}(x_0)O^{(d)}_{2b,j}(0)\rangle, \tag{12}$$

where $d \in \mathbb{Z}$ is related to the center of mass momentum by $P = \frac{2\pi}{L}d$, and the two-particle operators are constructed by

$$O^{(d)}_{2b,n}(x_0) = \tilde{\phi}_n(x_0)\tilde{\phi}_{d-n}(x_0). \tag{13}$$

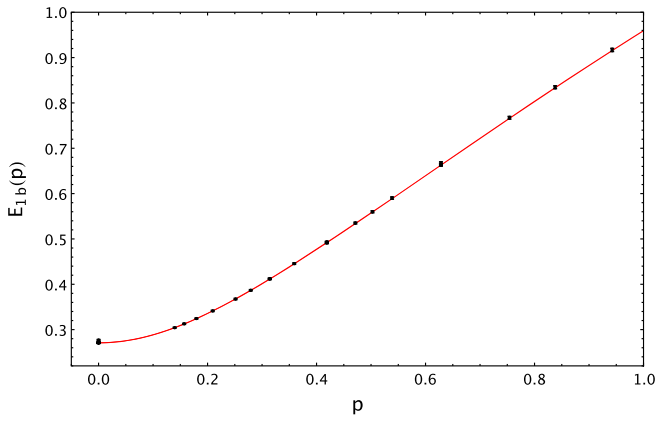


FIG. 4. Plot of single-particle spectra in various lattices from $L = 10$ up to $L = 45$ vs lattice dispersion relation (red band), $E_{1b}(p) = \cosh^{-1}(\cosh m + 1 - \cos p)$, where $p = \frac{2\pi}{L}n, n \in \mathbb{Z}$.

Four two-particle operators are used in our simulation: $n = (0, 1, 2, 3)$, so the size of the matrix of the two-particle correlation functions is $4 \times 4$, $3 \times 3$, and $2 \times 2$ for $d = 0$, 1, 2, respectively.

The spectral decomposition of the correlation function matrices is usually given by

$$C^{(d)}_{2b,(i,j)}(x_0) = \sum_n v^{(d,n)*}_{2b,i} v^{(d,n)}_{2b,j} e^{-E^{(d)}_{2b,n} x_0}, \tag{14}$$

where $v^{(d,n)}_{2b,i} = \langle n|O^{(d)}_{2b,i}(0)|0\rangle$, and $n$ labels the $n$th energy eigenstate $E^{(d)}_{2b,n}$. In order to extract excited energy states, a generalized eigenvalue method [73] is proposed:

$$C^{(d)}_{2b}(x_0)\xi_{2b,n} = \lambda^{(d)}_{2b,n}(x_0, \bar{x}_0) C^{(d)}_{2b}(\bar{x}_0)\xi_{2b,n}, \tag{15}$$

where $\bar{x}_0$ is a small reference time. Mixing of multiparticle states is protected by the conservation of charge quantum number in the complex $\phi^4$ model. Also, diagonalized correlation functions barely show the contamination of higher energy states in $\lambda^{(d)}_{2b,n}(x_0, \bar{x}_0)$; see Figs. 1 and 2. Therefore, $\bar{x}_0$ is set to zero and a simple form of $\lambda^{(d)}_{2b,n}(x_0, 0) = e^{-E^{(d)}_{2b,n} x_0}$ is used in the data fitting for $x_0 \in [0, 10]$. The two-particle spectra for various lattice sizes and $d$ are presented in Fig. 5.

The phase shift of two-body scattering is extracted from two-particle energy levels, $E^{(d)}_{2b,n}$, by using the relation

$$\delta^{(d)}_{\text{lat}}(k) = -\frac{kL}{2} - \frac{\pi}{2} d, \tag{16}$$

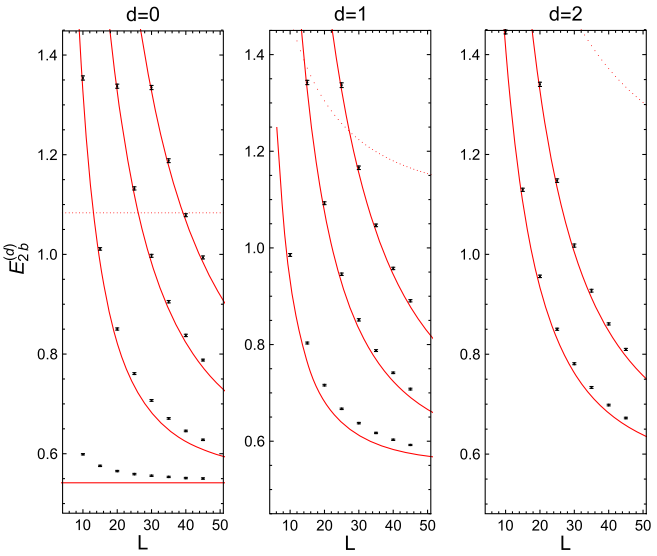


FIG. 5. Plot of two-particle spectra from various lattice sizes from $L = 10$ up to $L = 45$ and for $d = 0, 1, 2$ vs free two-particle energy levels (red curve): $E_{2b}(L) = \sum_{i=1,2} \cosh^{-1}(\cosh m + 1 - \cos p_i)$, where $p_i = \frac{2\pi}{L} n_i$, $n_i \in \mathbb{Z}$. Dotted curves represent the four-particle threshold.

where the relative momentum of two particles, $k$, is given by the solutions of the two-particle energy-momentum dispersion relation

$$E^{(d)}_{2b}(L) = \sum_{i=1,2} \cosh^{-1}(\cosh m + 1 - \cos p_i), \tag{17}$$

where $p_1 = \frac{\pi}{L} d + k$ and $p_2 = \frac{\pi}{L} d - k$; see the extracted phase shift in Fig. 6. The exact expression of the phase shift,

$$\delta(k) = \cot^{-1}\left(-\frac{2k}{mV_0}\right), \tag{18}$$

is used to fit the lattice results, $\delta^{(d)}_{\text{lat}}(k)$, and to fix the coupling strength, $V_0$. We thus find $mV_0 = 0.170 \pm 0.015$.

### C. Three-particle spectra

For three-particle operators with $d = 0$, 1, 2, four operators are used in the present work:

$$O^{(d)}_{3b,n}(x_0) = \tilde{\phi}_n(x_0)\tilde{\phi}_{-n}(x_0)\tilde{\phi}_d(x_0), \quad n = 0, 1, 2, \tag{19}$$

and

$$\begin{aligned} O^{(d=0)}_{3b,3}(x_0) &= \tilde{\phi}_1(x_0)\tilde{\phi}_1(x_0)\tilde{\phi}_{-2}(x_0), \\ O^{(d=1)}_{3b,3}(x_0) &= \tilde{\phi}_0(x_0)\tilde{\phi}_{-1}(x_0)\tilde{\phi}_2(x_0), \\ O^{(d=2)}_{3b,3}(x_0) &= \tilde{\phi}_0(x_0)\tilde{\phi}_1(x_0)\tilde{\phi}_1(x_0). \end{aligned} \tag{20}$$

Similar to the two-particle correlation function matrix, the matrix element of the three-particle correlation function is given by

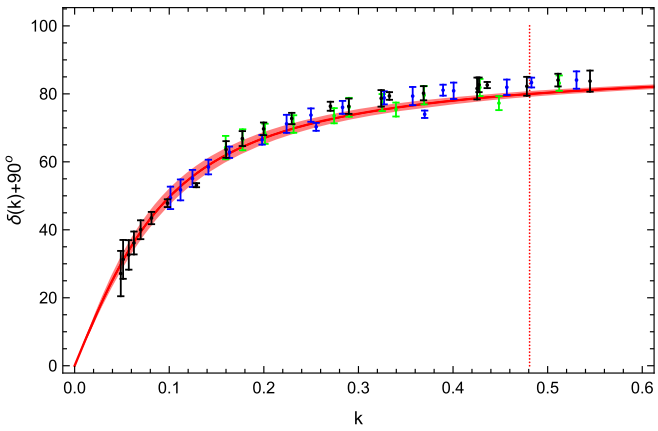


FIG. 6. Two-particle scattering phase shift $\delta^{(d)}_{\text{lat}}(k)$ from various lattices and several moving frames, $d = 0$ (black), $d = 1$ (blue), and $d = 2$ (green), vs the fitting result (red band) by using the expression $\delta(k) = \cot^{-1}(-\frac{2k}{mV_0})$. The vertical line symbolizes the four-particle threshold.

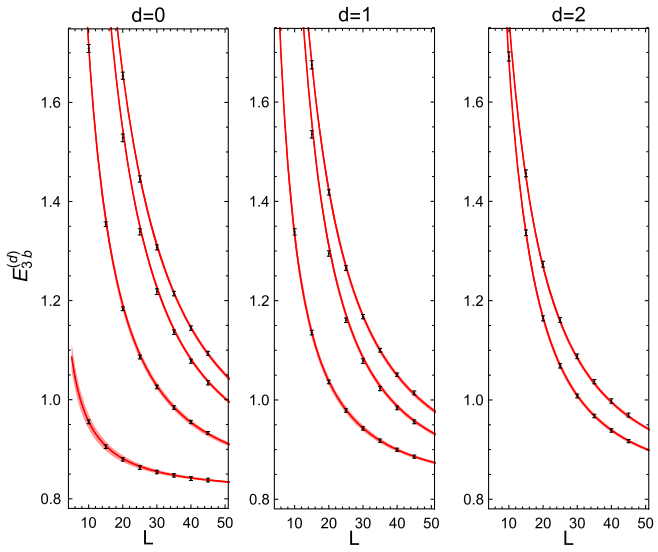


FIG. 7. Three-particle spectra from various lattice size s from $L = 10$ up to $L = 45$ and for $d = 0$, 1, 2 vs predicted three-particle energy levels (red band): $E_{3b}(L) = \sum_{i=1}^{3} \cosh^{-1}(\cosh m + 1 - \cos p_i)$, where $p_3 = \frac{2\pi}{L} d - p_1 - p_2$, and the values of $p_1$ and $p_2$ are given by the solutions of the three-body quantization conditions in Eq. (4).

$$C_{3b,(i,j)}^{(d)}(x_0) = \langle O_{3b,i}^{(d)*}(x_0) O_{3b,j}^{(d)}(0) \rangle. \tag{21}$$

In the two-particle sector, the generalized eigenvalue method is also applied to extract three-body energy levels,

$$C_{3b}^{(d)}(x_0)\xi_{3b,n} = \lambda_{3b,n}^{(d)}(x_0, 0) C_{3b}^{(d)}(0)\xi_{3b,n}, \tag{22}$$

where $\lambda_{3b,n}^{(d)}(x_0, 0) = e^{-E_{3b,n}^{(d)} x_0}$. An example of the three-particle correlation function, $\lambda_{3b,n}^{(d)}(x_0, 0)$, and effective mass, $\ln[\lambda_{3b,n}^{(d)}(x_0, 0)/\lambda_{3b,n}^{(d)}(x_0 + 1, 0)]$, is given in Figs. 1 and 2.

Given the values of particle mass, $m$, and coupling strength, $V_0$, that we learned from discussion in previous sections, three-particle spectra do not provide any new insight into the fundamental parameters of $\phi^4$ theory due to the absence of a three-body force. However, in general, three-particle spectra are still considered a useful tool to explore and understand the dynamics of three-particle interaction. In reality, the spectra also provide opportunities to investigate the possibility of more fundamental parameters of lattice QCD theory. Nevertheless, since the exact solutions are known, we only tend to demonstrate the consistence of predicted three-particle spectra compared to simulation results. The predicted three-particle spectra are determined by three-body energy-momentum dispersion relations in terms of two independent particle momenta, say, $p_1$ and $p_2$,

$$E_{3b}^{(d)}(L) = \sum_{i=1}^{3} \cosh^{-1}(\cosh m + 1 - \cos p_i), \tag{23}$$

where $p_3 = \frac{2\pi}{L} d - p_1 - p_2$. Two independent particle momenta, $p_1$ and $p_2$, are the solutions of the three-body quantization conditions given in Eq. (4). The main results of the three-particle spectra are presented in Fig. 7. As we can see, the agreement of predicted spectra against simulation results is quite remarkable.

## V. SUMMARY

In summary, the lattice simulation of multiparticle interaction is studied by using a complex $\phi^4$ lattice model. The simulation is performed in $(1 + 1)$-dimensional space and time for various sizes of lattices and multiple moving frames. The two-dimensional $\phi^4$ model is exactly solvable and analytical expressions of multiparticle quantization conditions are known in a finite volume [64]. This feature makes it a perfect test bed for studying multiparticle interaction in a lattice. The typical 3–4 numbers of multiparticle operators are used in our simulation, and a variational approach is implemented to extract excited state energy levels. Two parameters of $\phi^4$ theory, single-particle mass and coupling strength, are extracted from single-particle and two-particle spectra, respectively. Then, extracted $\phi^4$ theory parameters are applied to predict three-particle spectra by using analytical three-body quantization conditions compared with three-particle spectra from simulations. Predicted three-particle spectra and lattice results show quite remarkable agreement.

## ACKNOWLEDGMENTS

We acknowledge support from the Department of Physics and Engineering, California State University, Bakersfield, CA. We also thank Vladimir Gasparian and David Gross for numerous fruitful discussions. This research was supported in part by the National Science Foundation under Grant No. NSF PHY-1748958.

[1] J. G. Taylor, Phys. Rev. **150**, 1321 (1966).
[2] J.-L. Basdevant and R. E. Kreps, Phys. Rev. **141**, 1398 (1966).
[3] F. Gross, Phys. Rev. C **26**, 2226 (1982).
[4] L. D. Faddeev, Zh. Eksp. Teor. Fiz. **39**, 1459 (1960) [Sov. Phys. JETP **12**, 1014 (1961)].
[5] L. D. Faddeev, *Mathematical Aspects of the Three-Body Problem in the Quantum Scattering Theory* (Israel Program for Scientific Translation, Jerusalem, Israel, 1965).
[6] W. Glöckle, *The Quantum Mechanical Few-Body Problem* (Springer, Berlin, Germany, 1983).
[7] A. C. Phillips, Phys. Rev. **142**, 984 (1966).
[8] D. V. Fedorov and A S. Jensen, Phys. Rev. Lett. **71**, 4103 (1993).
[9] W. Glöckle, H. Witala, D. Hüber, H. Kamada, and J. Golak, Phys. Rep. **274**, 107 (1996).
[10] N. N. Khuri and S. B. Treiman, Phys. Rev. **119**, 1115 (1960).
[11] J. B. Bronzan and C. Kacser, Phys. Rev. **132**, 2703 (1963).
[12] I. J. R. Aitchison, Il Nuovo Cimento **35**, 434 (1965).
[13] I. J. R. Aitchison, Phys. Rev. **137**, B1070 (1965); Phys. Rev. **154**, 1622 (1967).
[14] I. J. R. Aitchison and R. Pasquier, Phys. Rev. **152**, 1274 (1966).
[15] R. Pasquier and J. Y. Pasquier, Phys. Rev. **170**, 1294 (1968).
[16] R. Pasquier and J. Y. Pasquier, Phys. Rev. **177**, 2482 (1969).
[17] P. Guo, I. V. Danilkin, and A. P. Szczepaniak, Eur. Phys. J. A **51**, 135 (2015).
[18] P. Guo, Phys. Rev. D **91**, 076012 (2015).
[19] I. V. Danilkin, C. Fernández-Ramírez, P. Guo, V. Mathieu, D. Schott, and A. P. Szczepaniak, Phys. Rev. D **91**, 094029 (2015).
[20] P. Guo, Mod. Phys. Lett. A **31**, 1650058 (2016).
[21] J. Kambor, C. Wiesendanger, and D. Wyler, Nucl. Phys. **B465**, 215 (1996).
[22] A. V. Anisovich and H. Leutwyler, Phys. Lett. B **375**, 335 (1996).
[23] G. Colangelo, S. Lanz, and E. Passemar, Proc. Sci., CD09 (**2009**) 047.
[24] S. Lanz, Proc. Sci., CD12 (**2013**) 007.
[25] S. P. Schneider, B. Kubis, and C. Ditsche, J. High Energy Phys. 02 (2011) 028.
[26] K. Kampf, M. Knecht, J. Novotny, and M. Zdrahal, Phys. Rev. D **84**, 114015 (2011).
[27] P. Guo, I. V. Danilkin, D. Schott, C. Fernández-Ramírez, V. Mathieu, and A. P. Szczepaniak, Phys. Rev. D **92**, 054016 (2015).
[28] P. Guo, I. V. Danilkin, C. Fernández-Ramírez, V. Mathieu, and A. P. Szczepaniak, Phys. Lett. B **771**, 497 (2017).
[29] S. Aoki *et al.* (CP-PACS Collaboration), Phys. Rev. D **76**, 094506 (2007).
[30] K. Sasaki and N. Ishizuka, Phys. Rev. D **78**, 014511 (2008).
[31] X. Feng, K. Jansen, and D. B. Renner, Phys. Rev. D **83**, 094505 (2011).
[32] J. J. Dudek, R. G. Edwards, M. J. Peardon, D. G. Richards, and C. E. Thomas (Hadron Spectrum Collaboration), Phys. Rev. D **83**, 071504 (2011).
[33] S. R. Beane, E. Chang, W. Detmold, H. W. Lin, T. C. Luu, K. Orginos, A. Parreño, M. J. Savage, A. Torok, and A. Walker-Loud (NPLQCD Collaboration), Phys. Rev. D **85**, 034505 (2012).
[34] C. B. Lang, D. Mohler, S. Prelovsek, and M. Vidmar, Phys. Rev. D **84**, 054503 (2011).
[35] S. Aoki *et al.* (CS Collaboration), Phys. Rev. D **84**, 094505 (2011).
[36] J. J. Dudek, R. G. Edwards, and C. E. Thomas (Hadron Spectrum Collaboration), Phys. Rev. D **86**, 034031 (2012).
[37] J. J. Dudek, R. G. Edwards, and C. E. Thomas, Phys. Rev. D **87**, 034505 (2013).
[38] D. J. Wilson, J. J. Dudek, R. G. Edwards, and C. E. Thomas, Phys. Rev. D **91**, 054008 (2015).
[39] D. J. Wilson, R. A. Briceno, J. J. Dudek, R. G. Edwards, and C. E. Thomas, Phys. Rev. D **92**, 094502 (2015).
[40] J. J. Dudek, R. G. Edwards, and D. J. Wilson (Hadron Spectrum Collaboration), Phys. Rev. D **93**, 094506 (2016).
[41] M. Lüscher, Nucl. Phys. **B354**, 531 (1991).
[42] K. Rummukainen and S. Gottlieb, Nucl. Phys. **B450**, 397 (1995).
[43] C.-J. D. Lin, G. Martinelli, C. T. Sachrajda, and M. Testa, Nucl. Phys. **B619**, 467 (2001).
[44] N. H. Christ, C. Kim, and T. Yamazaki, Phys. Rev. D **72**, 114506 (2005).
[45] V. Bernard, Ulf-G. Meißner, and A. Rusetsky, Nucl. Phys. **B788**, 1 (2008).
[46] V. Bernard, M. Lage, Ulf-G. Meißner, and A. Rusetsky, J. High Energy Phys. 08 (**2008**) 024.
[47] S. He, X. Feng, and C. Liu, J. High Energy Phys. 07 (2005) 011.
[48] M. Lage, Ulf-G. Meißner, and A. Rusetsky, Phys. Lett. B **681**, 439 (2009).
[49] M. Döring, Ulf-G. Meißner, E. Oset, and A. Rusetsky, Eur. Phys. J. A **47**, 139 (2011).
[50] S. Aoki, N. Ishii, T. Doi, T. Hatsuda, Y. Ikeda, T. Inoue, K. Murano, H. Nemura, and K. Sasaki (HAL QCD Collaboration), Proc. Jpn. Acad. Ser. B **87**, 509 (2011).
[51] R. A. Briceno and Z. Davoudi, Phys. Rev. D **88**, 094507 (2013).
[52] M. T. Hansen and S. R. Sharpe, Phys. Rev. D **86**, 016007 (2012).
[53] P. Guo, J. Dudek, R. Edwards, and A. P. Szczepaniak, Phys. Rev. D **88**, 014501 (2013).
[54] S. Kreuzer and H.-W. Hammer, Phys. Lett. B **673**, 260 (2009).
[55] S. Kreuzer and H.-W. Hammer, Eur. Phys. J. A **43**, 229 (2010).
[56] S. Kreuzer and H.-W. Hammer, Eur. Phys. J. A **48**, 93 (2012).
[57] K. Polejaeva and A. Rusetsky, Eur. Phys. J. A **48**, 67 (2012).
[58] R. A. Briceno and Z. Davoudi, Phys. Rev. D **87**, 094507 (2013).
[59] M. T. Hansen and S. R. Sharpe, Phys. Rev. D **90**, 116003 (2014).
[60] M. T. Hansen and S. R. Sharpe, Phys. Rev. D **92**, 114509 (2015).
[61] M. T. Hansen and S. R. Sharpe, Phys. Rev. D **93**, 096006 (2016).
[62] H.-W. Hammer, J.-Y. Pang, and A. Rusetsky, J. High Energy Phys. 09 (2017) 109.

[63] H.-W. Hammer, J.-Y. Pang, and A. Rusetsky, J. High Energy Phys. 10 (2017) 115.
[64] P. Guo, Phys. Rev. D **95**, 054508 (2017).
[65] P. Guo and V. Gasparian, Phys. Lett. B **774**, 441 (2017).
[66] Ulf-G. Meißner, G. Rios, and A. Rusetsky, Phys. Rev. Lett. **114**, 091602 (2015); **117**, 069902(E) (2016).
[67] R. A. Briceno, M. T. Hansen, and S. R. Sharpe, Phys. Rev. D **95**, 074510 (2017).
[68] S. R. Sharpe, Phys. Rev. D **96**, 054515 (2017).
[69] M. Mai and M. Döring, Eur. Phys. J. A **53**, 240 (2017).
[70] P. Guo and V. Gasparian, Phys. Rev. D **97**, 014504 (2018).
[71] F. Romero-Löpez, A. Rusetsky, and C. Urbach, Eur. Phys. J. C **78**, 846 (2018).
[72] C. Michael, Nucl. Phys. **B259**, 58 (1985).
[73] M. Luscher and U. Wolff, Nucl. Phys. **B339**, 222 (1990).
[74] B. Blossier, M. Della Morte, G. von Hippel, T. Mendes, and R. Sommer, J. High Energy Phys. 04 (2009) 094.
[75] H. B. Thacker, Phys. Rev. D **11**, 838 (1975).
[76] J. B. McGuire, J. Math. Phys. (N.Y.) **5**, 622 (1964).
[77] C. N. Yang, Phys. Rev. Lett. **19**, 1312 (1967).
[78] H. A. Bethe, Z. Phys. **71**, 205 (1931).
[79] E. H. Lieb and W. Liniger, Phys. Rev. **130**, 1605 (1963).
[80] P. Guo, Phys. Rev. D **88**, 014507 (2013).
[81] S. Duane, A. D. Kennedy, B. J. Pendleton, and D. Roweth, Phys. Lett. B **195**, 216 (1987).
[82] S. Duane and J. B. Kogut, Nucl. Phys. **B275**, 398 (1986).
[83] C. R. Gattringer and C. B. Lang, Nucl. Phys. **B391**, 463 (1993).